nature materials

SUPPLEMENTARY INFORMATION

DOI: 10.1038/NMAT4836

In the format provided by the authors and unedited.

A charge density wave-like instability in a doped spin–orbit-assisted weak Mott insulator

H. Chu[1,2], L. Zhao[2,3], A. de la Torre[2,3], T. Hogan[4], S.D. Wilson[4] & D. Hsieh[2,3]

[1]Department of Applied Physics, California Institute of Technology, Pasadena, CA 91125, USA

[2]Institute for Quantum Information and Matter, California Institute of Technology, Pasadena, CA 91125, USA

[3]Department of Physics, California Institute of Technology, Pasadena, CA 91125, USA

[4]Materials Department, University of California, Santa Barbara, CA 93106, USA

S1. Fits of $Sr_3Ir_2O_7$ reflectivity transients to a single exponential decay

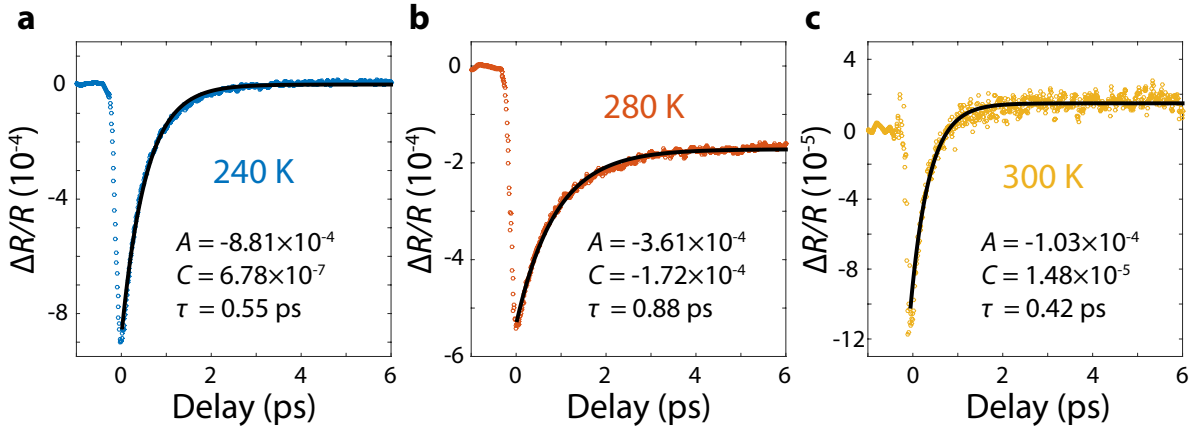

FIG. S1. Representative best fits of the reflectivity transients (open circles) of $Sr_3Ir_2O_7$ to a single exponential decay (solid lines) at temperatures **a,** below (T = 240 K), **b,** at (T = 280 K) and **c,** above (T = 300 K) the Néel temperature. The values of the best fit parameters are displayed in each panel.

The reflectivity transients of $Sr_3Ir_2O_7$ at all temperatures shown in Fig. 1a of the main text are well described by a single exponential decay function $\Delta R/R = Ae^{-t/\tau}+C$, where A is the amplitude of the pump induced fractional change in reflectivity and τ is the characteristic electron-phonon relaxation time. Relaxation processes that are much slower than τ, such as heat diffusion away from the probed region, are approximated as being constant (C) over the time interval of interest. Fits were constrained between delay times of 0.1 ps and 6 ps for all temperatures and the typical quality of fit is shown in Fig. S1.

S2. Fits of $A(T)$ and $\tau(T)$ to photo-excited e-h pair relaxation model

Analytical expressions for the temperature dependence of the amplitude $A(T)$ and relaxation time $\tau(T)$ of the reflectivity transients of a fully gapped (nodeless) system below its gap opening temperature were derived in Ref.[1] and are shown below.

$$A(T) \propto \frac{\frac{F}{\Delta(T)+k_BT/2}}{1+\gamma\sqrt{\frac{2k_BT}{\pi\Delta(T)}}\exp(-\frac{\Delta(T)}{k_BT})}$$

$$\tau \propto \frac{1}{\Delta(T)}$$

Here F is the fluence of the pump pulse, k_B is Boltzmann's constant and γ is a phenomenological fitting parameter. Although the derivation was made in the context of the recombination of quasiparticles across a superconducting gap, the same formalism extends to and is often used to describe the recombination of electron-hole pairs across an insulating gap.

To fit the data shown in Fig. 1b of the main text, we used a value $F = 80\ \mu\text{J/cm}^2$ and assumed a BCS-like temperature dependence of the insulating gap $\Delta(T) = \Delta_0\sqrt{1-T/T_N}$. The zero temperature gap magnitude Δ_0, Néel temperature T_N and γ were left as free parameters. Fits were constrained between temperatures of 180 K and 275 K. The best fits shown in Fig. 1b of the main text yielded the values $T_N = 280$ K, $\Delta_0 = 230$ meV and $\gamma = 12.2$. We note that this simple model produces the correct value of T_N but slightly overestimates the value of Δ_0.

S3. Fits of $(Sr_{1-x}La_x)_3Ir_2O_7$ reflectivity transients to a damped sinusoid

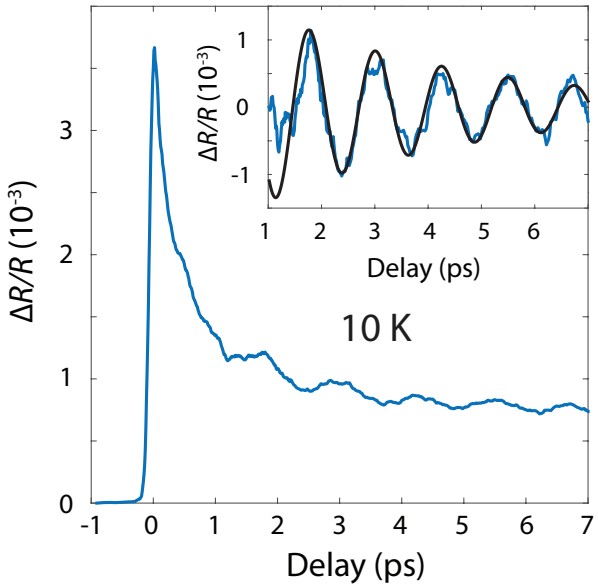

FIG. S2. Reflectivity transient of $(Sr_{1-x}La_x)_3Ir_2O_7$ with $x = 5.8$ % measured at 10 K reproduced from Fig. 3a of the main text. Inset shows the background subtracted data (blue line) overlaid with a best fit to a damped sinusoid (black line).

To extract the amplitude A_{DW}, temporal period τ_{DW} and damping rate Γ of the low frequency reflectivity modulations in metallic $(Sr_{1-x}La_x)_3Ir_2O_7$, we first subtracted a smoothly decaying background from the reflectivity transients and then fit the residual to a damped sinusoid of the form $A_{DW}e^{-\Gamma t}\sin(2\pi t/\tau_{DW} + \phi)$, where ϕ is a phase offset. Fits were constrained to the delay interval between 1.5 ps and 6 ps. The quality of fit for the $x = 5.8$ % sample measured at 10 K is shown in Fig. S2, which is typical of all other temperatures and doping levels studied.

S4. Fluence dependence of electronic mode in $(Sr_{1-x}La_x)_3Ir_2O_7$

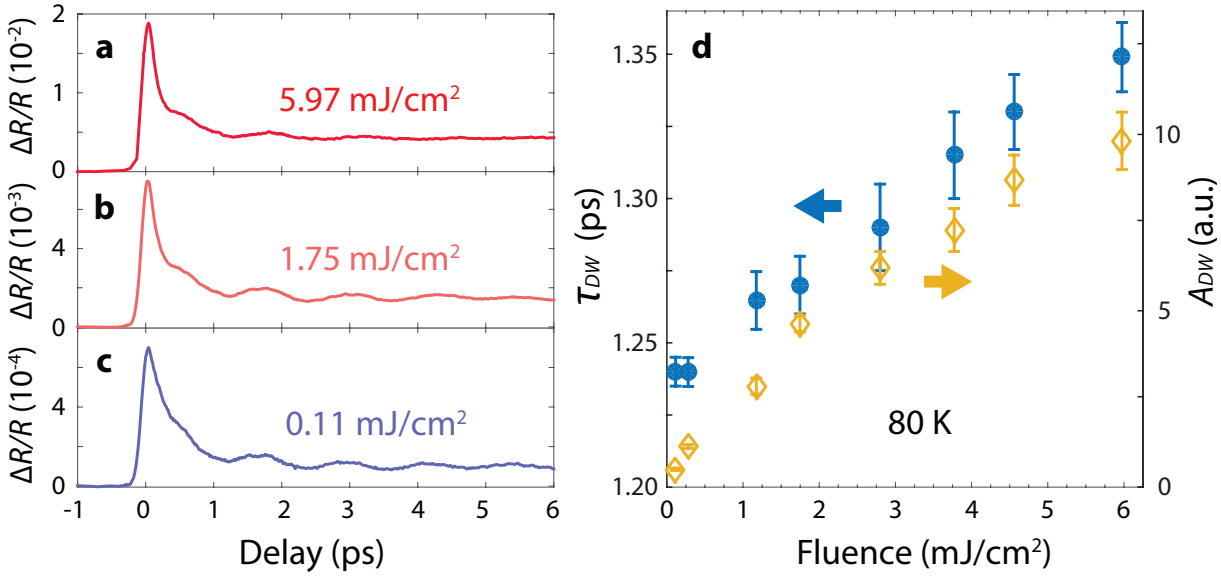

FIG. S3. Reflectivity transients of $(Sr_{1-x}La_x)_3Ir_2O_7$ with $x = 5.8$ % measured at 80 K with a pump fluence of **a,** 5.97 mJ/cm^2, **b,** 1.75 mJ/cm^2 and **c,** 0.11 mJ/cm^2. **d,** The pump fluence dependence of the period τ_{DW} (filled circles) and amplitude A_{DW} (open diamonds) of the reflectivity modulations observed in panels **a,** to **c,** extracted using the procedure described in section S3. Error bars represent the 95% confidence intervals of the fitted values.

To determine the pump fluence dependence of the low frequency reflectivity modulations in metallic $(Sr_{1-x}La_x)_3Ir_2O_7$, we measured the reflectivity transients of an $x = 5.8$ % doped sample at a temperature far below T_{DW} using a wide range of different pump fluences. As shown in Figs S3a-c, there is no qualitative change in the lineshape of the reflectivity transients over a roughly 50 fold increase in pump fluence. By fitting background subtracted reflectivity transients at different fluences to a damped sinusoid using the procedure described in section S3, we found that both the amplitude A_{DW} and period τ_{DW} of the reflectivity modulations increase monotonically with pump fluence (Fig. S3d). This is consistent with amplitude oscillations of an electronic order parameter and contrasts with the pump fluence dependence of the A_{1g} phonon mode, which grows in amplitude but does not noticeably shift in frequency as the pump fluence is raised.

S5. La-doping dependence of τ_{DW}

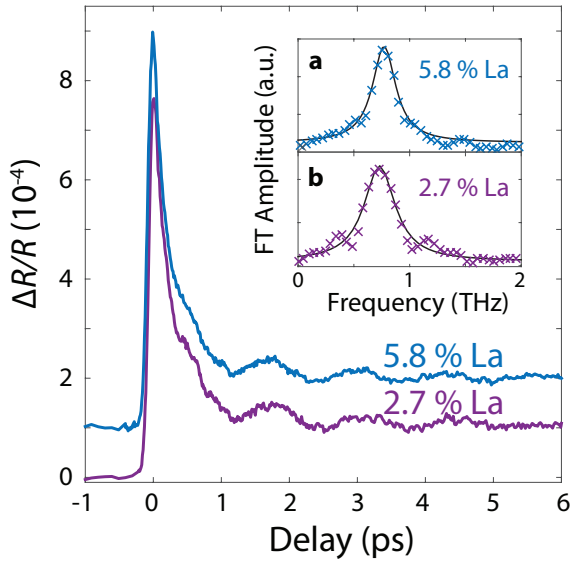

FIG. S4. Reflectivity transients of $x = 5.8$ % and $x = 2.7$ % doped $(Sr_{1-x}La_x)_3Ir_2O_7$ crystals measured at 100 K. Traces are vertically offset and scaled to similar magnitude for ease of comparison. Insets show the Fourier transforms of the background subtracted reflectivity transients of the **a,** $x = 5.8$ % and **b,** $x = 2.7$ % doped samples overlaid with fits to a Lorentzian function.

The temporal period τ_{DW} of the low frequency reflectivity modulations in metallic $(Sr_{1-x}La_x)_3Ir_2O_7$ is similar across all doping levels studied for any given temperature. As an example, Fig. S4 shows traces from metallic samples with the lowest ($x = 2.7$ %) and highest ($x = 5.8$ %) doping levels measured at 100 K. It is clear from the raw data alone that τ_{DW} is very similar for the two doping levels. We compared these traces more quantitatively by subtracting a decaying background as described in section S3 and then taking a Fourier transform. As shown in the insets of Fig. S4, the oscillation frequencies are the same for the two doping levels within our experimental resolution.

S6. Characterization of structural distortion and T_s in $(Sr_{0.93}Ca_{0.07})_3Ir_2O_7$

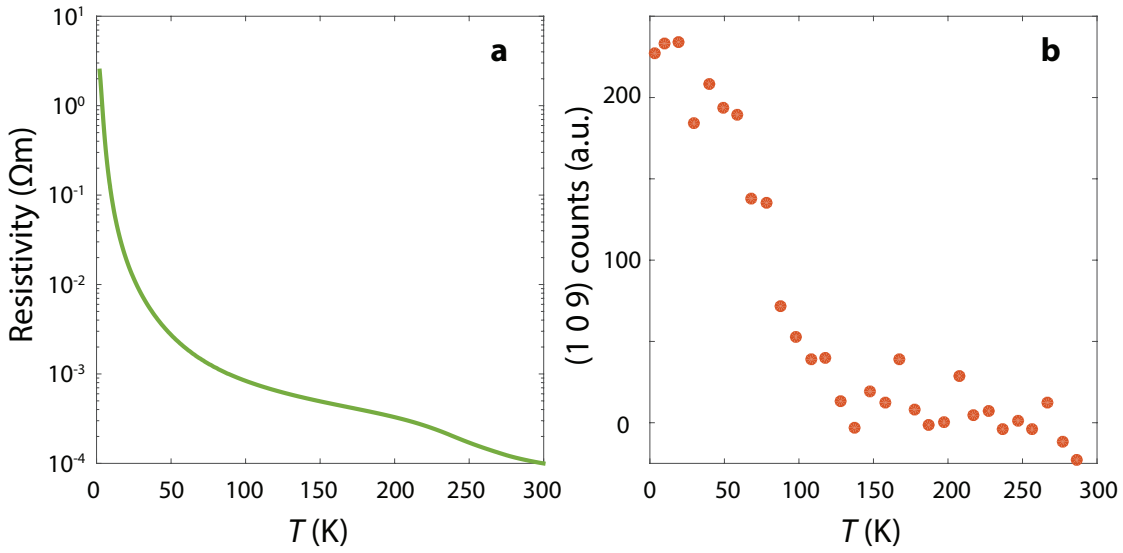

FIG. S5. Temperature dependence of **a,** the resistivity and **b,** the (1 0 9) structural Bragg peak measured by neutron diffraction of $(Sr_{0.93}Ca_{0.07})_3Ir_2O_7$.

The electrical properties of $(Sr_{0.93}Ca_{0.07})_3Ir_2O_7$ crystals from the same batch used in our study (see Fig. 4 of main text) were characterized by resistivity measurements, which were performed with a Lake Shore 370 AC Bridge using a four-probe lead configuration. A clear insulating behaviour that is similar to $Sr_3Ir_2O_7$ is observed (Fig. S5a), confirming the absence of a Fermi surface. The structural properties were characterized by neutron diffraction performed on the N5 triple-axis spectrometer at the Canadian Neutron Beam Centre at the Chalk River Laboratories. Like the case in metallic $(Sr_{1-x}La_x)_3Ir_2O_7$ samples, the weak structural distortion that occurs below T_s in insulating $(Sr_{0.93}Ca_{0.07})_3Ir_2O_7$ samples appears in the form of very low intensity Bragg peaks at *Bbcb* space group forbidden (h = odd, 0, l = odd) positions. In particular, the array of peaks detected in the Ca-substituted system, namely (1, 0, 3), (1, 0, 7), (3, 0, 3) and (1, 0, 9), were also detected in the La-doped system, supporting the equivalence of the two structural distortions. The value of $T_s \sim 120$ K in $(Sr_{0.93}Ca_{0.07})_3Ir_2O_7$ was determined through the temperature dependence of the background subtracted (1 0 9) nuclear Bragg peak as shown in Fig. S5b.

These data sets collected from $(Sr_{0.93}Ca_{0.07})_3Ir_2O_7$ are reproduced from those shown in [2], where further details of the sample characterization can be found.

S7. Magnon and spin-orbit exciton mode energies in $(Sr_{1-x}La_x)_3Ir_2O_7$

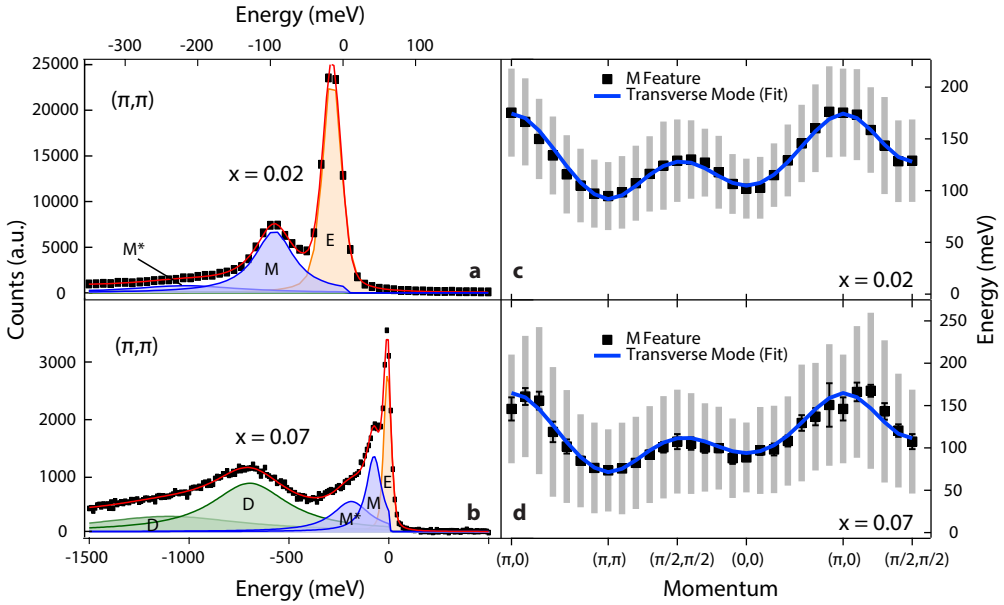

FIG. S6. (Reproduced from [3]). Ir L_3 edge (11.215 keV) RIXS energy scans collected at T = 40 K at a fixed momentum of (π,π) for $(Sr_{1-x}La_x)_3Ir_2O_7$ samples with **a,** $x = 0.02$ and **b,** $x = 0.07$. Features labeled E, M, M* and D denote scattering from the elastic line, single magnon, multimagnon and spin-orbital exciton respectively. Dispersion of the M feature for **c,** $x = 0.02$ and **d,** $x = 0.07$ samples based on fitting to Lorentzian functions [3] are plotted as squares with accompanying fitting errors shown in gray. Solid lines denote fits to a bond operator model as described in [3].

Although the static long-range antiferromagnetic order observed in the parent compound $Sr_3Ir_2O_7$ is suppressed in the La-doped metallic samples, its remnant 2D magnetic fluctuations can still survive in the metallic regime. In order to study the possibility that the low energy mode observed using time-resolved optical reflectivity originates from coherent oscillations of such a fluctuating magnetic order parameter, we measured the dispersion of magnon excitations in $(Sr_{1-x}La_x)_3Ir_2O_7$ using resonant inelastic x-ray scattering (RIXS) at the Ir L_3 edge. A previous RIXS study of the parent compound $Sr_3Ir_2O_7$ [4] has shown that its excitation (magnon) spectrum is fully gapped, with the smallest gap size of $\Delta_{mag} \sim 90$ meV (= 22 THz) occurring at the (π,π) point in the Brillouin zone. Upon La-doping, our RIXS data shows that these magnon excitations persist (see features labeled M in Fig. S6a,b)

across the insulator-to-metal transition ($x_c \sim 0.02$) even though static long-range magnetic order is suppressed. By tracking the momentum dependence of this M feature in the RIXS spectra, we obtained the magnon dispersion relations (Fig. S6c,d) showing that the gap at (π,π) in the $x = 0.02$ ($\Delta_{mag} \sim 90$ meV = 22 THz) and $x = 0.07$ ($\Delta_{mag} \sim 70$ meV = 17 THz) samples stays at a value comparable to that observed in the parent compound. Since the frequency of the mode observed in our time-resolved optical reflectivity measurements (~ 1 THz) is far lower than the lowest energy magnon across all La-doping values measured, we rule out a magnon origin of this mode.

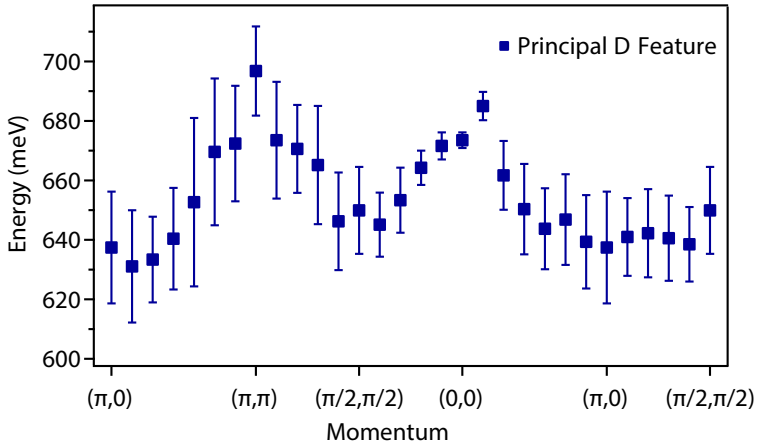

FIG. S7. Dispersion of the spin-orbit exciton mode in the metallic $x = 0.07$ sample (see feature labeled D in Fig. S6**b**) obtained by fitting the RIXS data to Lorentzian functions [3] are plotted as squares with accompanying fitting errors.

We also studied the possibility that the mode observed by time-resolved optical reflectivity originates from a charge neutral spin-orbit exciton mode (a bound state of a $J_{eff} = 3/2$ hole and a $J_{eff} = 1/2$ electron) that has very recently been observed by RIXS in parent $Sr_3Ir_2O_7$ [5]. Optical conductivity measurements [6] have shown that the broad $J_{eff} = 3/2$ and $J_{eff} = 1/2$ manifolds in $Sr_3Ir_2O_7$ are separated in energy by approximately 0.8 eV and therefore $J_{eff} = 3/2$ to $J_{eff} = 1/2$ excitations are energetically accessible by our pump photons ($\hbar\omega = 1.5$ eV). Our RIXS measurements have also detected the spin-orbit exciton in metallic La-doped $Sr_3Ir_2O_7$ samples at this energy scale (see principal feature labeled D in Fig. S6b) and its complete dispersion relation is shown Fig. S7. As is the case with the magnon spectrum, the spin-orbit exciton mode is fully gapped with a gap energy scale of around 650 meV =

157 THz. Since this again far exceeds the frequency of the mode observed in time-resolved optical reflectivity, we can also rule this out as a possible origin.

---

[1] V. V. Kabanov *et al.*, *Phys. Rev.* B **59**, 1497-1506 (1999).

[2] T. Hogan *et al.*, *Phys. Rev. Lett.* **114**, 257203 (2015).

[3] T. Hogan *et al.*, *Phys. Rev.* B **94**, 100401(R) (2016).

[4] J. Kim *et al.*, *Phys. Rev. Lett.* **109**, 157402 (2012).

[5] Y. Ding *et al.*, *Phys. Rev. Lett.* **116**, 216402 (2016).

[6] H. J. Park *et al.*, *Phys. Rev.* B **89**, 155115 (2014).